

INTERACTION OF LASER RADIATION WITH MATTER. LASER PLASMA

PACS numbers: 52.50.Jm; 52.38.Mf; 79.20.Eb; 32.70.Jz
DOI: 10.1070/QE2012v042n11ABEH014969

Broadening of the spectral lines of a buffer gas and target substance in laser ablation

N.E. Kask, S.V. Michurin

Abstract. **The broadening of discrete spectral lines from the plasma produced in the laser ablation of metal targets in a broad pressure range (10^2–10^7 Pa) of the ambient gas (Ar, He, H_2) was studied experimentally. The behaviour of spectral line broadening for the buffer gases was found to be significantly different from that for the atoms and ions of the target material. In comparison with target atoms, the atoms of buffer gases radiate from denser plasma layers, and their spectral line profiles are complex in shape.**

Keywords: *laser ablation, percolation, Stark broadening of spectral lines.*

1. Introduction

The broadening of discrete lines observed in the spectrum of plasmas produced in the laser ablation of different targets has been the subject numerous experimental investigations. As a rule, these investigations are concerned with atomic and ionic spectra of the target substance, while data on the line broadening of the buffer gas surrounding the target are scarce in the literature. At the same time, in the diagnostics of laboratory plasmas quite often advantage is taken of the method based on studying the broadening and shifts of the spectral lines of specially introduced gases (hydrogen, helium, argon, etc.).

One of the objectives of the present work was to study and compare the broadening of spectral lines observed for buffer gas and target atoms. The buffer gas is in contact with the outer boundary of the plasma domain, and its composition and pressure affect not only the plasma parameters like the density, the temperature, and the degree of ionisation, but also the processes of condensation and clusterisation. Studying the intensity and broadening of the atomic spectral lines of the buffer gas results in a more detailed description of the processes occurring in laser ablation.

According to Ref. [1], a dense plasma with a temperature of several thousand kelvins may be the site of formation of 'hot' clusters: virtual atomic chains and fractal-like structures. The definition of 'hot' may also be used in reference to percolation clusters, both critical and subcritical, which emerge according to the dynamic percolation model [2, 3] in the dense plasma at the target surface. Ramified fractal structures with extensive inner surface also lead to a higher electron density in their vicinity as a result of the Richardson emission [4] and to an increase in local electric intensity at the branch ends. Furthermore, in the percolation clusters there emerge giant fluctuations of local light fields, according to Refs [5, 6].

Another subject of the present work is the effect of 'hot' clusters emerging in the ablation of metal targets on the width of spectral lines of inert buffer gases. Our experimental technique relied on the assumption that the buffer gas atoms which find themselves in the vicinity of a cluster, unlike the target atoms, do not enter into its composition and retain their discrete spectrum. Local field fluctuations in the cluster as well as the enhanced electron density may be responsible for a qualitative difference of the behaviour of the broadening and shift of the spectral lines of the buffer gas from that of the atoms and ions of the target substance.

2. Experimental facility and techniques employed

Metal targets were ablated under laser irradiation of different durations at a wavelength of 1.06 μm. Three regimes of irradiation were used: by a single pulse (LTIPCh-8) (regime 1), by a train of 7–10 pulses of nanosecond duration (a laser with a γ-LiF saturable absorber) (regime 2), and by a 10-ms pulse with an energy of ∼100 J (regime 3). The experiments with different durations of laser irradiation were performed for the purpose of determining the general properties as well as the features characteristic for specific time scales and light intensities. In the irradiation regime specifies above, the respective radii of caustics were equal to 0.25 ± 0.05 mm, 0.35 ± 0.06 mm, and ∼2 mm, and the averaged intensity values amounted to 4.5×10^9, 1.6×10^9 , and 3.2×10^5 W cm^{-2}. Laser radiation with an intensity approximately ten times higher than the target ablation threshold was used for target evaporation.

The target under investigation was placed in a leakproof chamber (the diameter and length of the interior cavity were equal to 25 and 150 mm). The pressure of a buffer gas in the chamber could be varied from 0.001 to 150 atm. For a buffer gas use was made both of pure gases (hydrogen, helium, and argon) and of their mixtures.

We investigated the spectrum and intensity of laser plasma radiation propagating in two directions: the longitudinal one – in the opposite direction to the laser flux, and in the transverse direction – perpendicular to the plume axis. In the latter case, we recorded the glow of the plasma layer located at a given distance from the target surface. The spatial resolution was equal to ∼100 μm. Time-integrated spectral were obtained using a spectrometer with a diffraction grating (600 grooves mm^{-1}, 10-μm slit width, spectral resolving power

N.E. Kask, S.V. Michurin D.V. Skobel'tsyn Institute of Nuclear Physics, M.V. Lomonosov Moscow State University, Vorob'evy gory, 119991 Moscow, Russia; e-mail: nek@srd.sinp.msu.ru

Received 30 July 2012
Kvantovaya Elektronika **42** (11) 1002–1007 (2012)
Translated by E.N. Ragozin

$\lambda/\delta\lambda \approx 24000$). The spectra were studied in the wavelength range $350 < \lambda < 900$ nm. The spectral width of the range under recording was determined by the focal distance F of the collecting camera lens. A lens with $F = 800$ mm projected a ~40-nm wide spectral interval on a linear CCD array. This lens was used for studying those spectral lines whose half-height width did not exceed 10 nm. To record broader lines, use was made of an $F = 120$ mm lens, which projected a ~270-nm wide interval on the linear CCD array. This interval is broad enough to contain spectral lines belonging to different objects: the atoms and ions of the target and the atoms of different buffer gases entering into the composition of the ambient atmosphere, which allowed us to compare the broadening and intensity of different lines in a specific experimental realisation.

The longitudinally directed glow integrated over the entire volume occupied by the plasma was directed to the input of an SFL-451 spectrofluorimeter, which had a spectral range $400 < \lambda < 900$ nm and a resolution of 6.4 nm. A comparison of the behaviour of the glow intensity in the transverse and longitudinal directions makes it possible to monitor the effects associated with the disintegration and aggregation of fractal structures, the formation and localisation of the absorption layer in peripheral plume layers and, in particular, the self-reversal of discrete lines.

Konjevic [7] formulated the following reliability criteria for plasma diagnostic techniques based on the measurements of the broadening and shift of spectral lines: uniformity of the plasma domain under study and its stationarity throughout the measurement time, the presence of local thermodynamic equilibrium (LTE); measurement of either the temperature or the density of electrons using some other experimental technique; and the inclusion of various mechanisms responsible for line broadening.

The plasma produced in the laser ablation by nanosecond pulses is characterised both by nonuniformity and nonstationarity, the LTE being violated near the surfaces across which gas-dynamic parameters experience discontinuities. The high substance density in the ablation cloud is accompanied with instabilities of different kind, intermittency, turbulence, etc. That is why in the execution of experimental investigations there is good reason to vary the laser exposure, the targets in use, and the parameters of the ambient atmosphere.

3. Experimental results and their discussion

3.1. Electron plasma temperature

In the majority of experimental works, laser ablation was investigated in the range of relatively low pressures of the gas surrounding the target ($p \leqslant 1$ atm). Since the percolation threshold is characterised by higher pressures [8], analysis of the processes accompanying this phenomenon generates a need for studying the electron plasma temperature (T_e) at gas pressures considerably higher than the atmospheric one. For instance, determining the density of plasma electrons from spectral line broadening requires knowledge about the temperature acquired using some other experimental technique.

The temperature T_e is usually estimated from the ratio of integral intensities of discrete spectral lines. The following spectral lines are frequently employed for this purpose in the spectrum of the plasma produced at the surface of a copper target: 510.55, 515.32, and 521.82 nm [9–12]. The expressions required for the calculations, which hold good in the presence of LTE, and the spectroscopic parameters for the transitions in atomic copper are given in Ref. [10].

In the ablation of a copper target by long pulses (regime 3), it is possible to determine the electron temperature realised in the stationary regime of plasma expansion. Figure 1 shows the glow of the laser plasma in the spectral interval containing the copper lines at the initial stage of discharge glow and 3 ms later. The buffer gas was argon at a pressure of 3 atm. In the course of exposure the spectral lines broaden, and there emerge dips at the peaks as a consequence of self-reversal. A conventional technique for calculating T_e leads to T_e(Cu,10 ms) ≈ 8500 ± 1000 K for each of the two spectra depicted in Fig. 1.

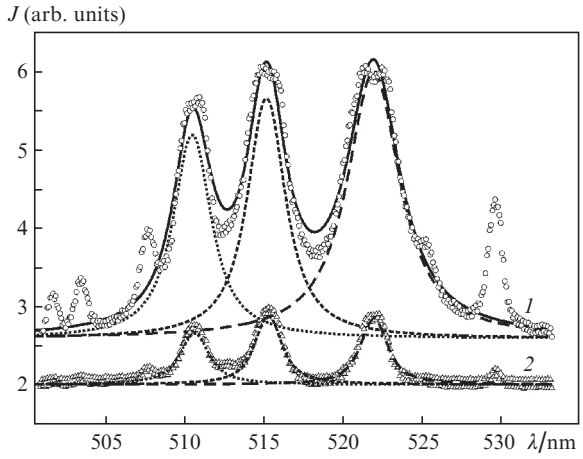

Figure 1. Glow spectrum of the laser plasma recorded when a copper target was exposed to a 10-ms long radiation pulse [(*1*) initial stage of discharge, (*2*) 3 ms later]. The circles represent experimental data, the dashed curves approximate separate lines by Lorentzian profiles, and the solid curve stands for their sum. The buffer gas is argon (3 atm).

The experimental data on the measurement of T_e obtained in the present work in the ablation of a copper target in regime 1 are collected in Figs 2 and 3. The data show the dependence of T_e on the distance of the plasma layer under study from the surface of the target, which is in the atmosphere of a buffer

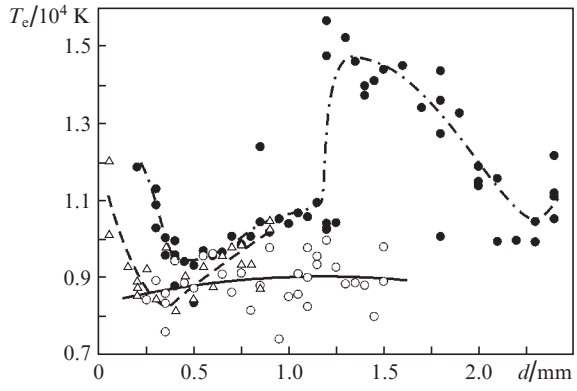

Figure 2. Electron plasma temperature T_e as a function of the distance d from the surface of a copper target at a pressure of the Ar buffer gas of 0.5 (●), 1.7 (○), and 15 atm (△) in regime 1. Uncertainty: 15%.

gas (He and Ar) at selected pressures. The solid curve corresponds to a pressure close to the percolation threshold. The dotted and dash-dotted curves illustrate the behaviour of the dependences for the pressures that are, respectively, higher and lower than the percolation threshold. As is clear from Figs 2 and 3, the electron temperature T_e becomes lower with increasing pressure, and the dependences show a dip at distances of 0.5–1.5 mm from the target surface, the intensity of continuum and discrete lines being highest in this case (see also Ref. [9]).

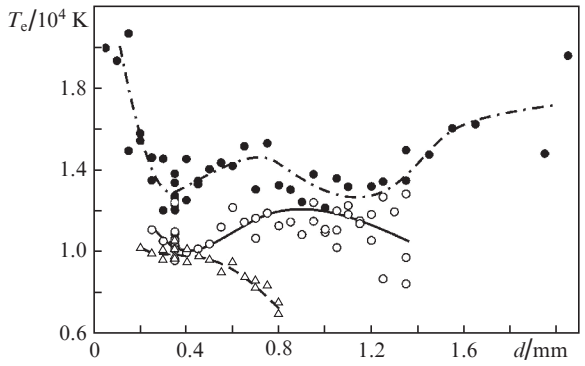

Figure 3. Electron plasma temperature T_e as a function of the distance d from the surface of a copper target at a pressure of the He buffer gas of 0.55 (●), 5 (○), and 70 atm (△) in regime 1. Uncertainty: 15%.

In Refs [9, 11, 12], the ablation of a copper target was effected with a single pulse at low buffer gas (Ar) pressures and temperature values were obtained, which are in agreement with the data given in Fig. 2. In our view, two results deserve discussion.

1. The ratio between the T_e value obtained for pulses of different duration. The irradiation intensity in regime 3 is approximately 10^4 times lower than in regime 1. Since the energy of electrons in the electric field of a light wave varies as the square root of the intensity, the proximity of the above value T_e(Cu, 10 ms) to the values given in Figs 2 and 3 testifies to significant changes in the mechanism of electron acceleration under long-pulse irradiation.

2. A dip in $T_e(d)$ dependences. The authors of Ref. [11] observed a blazing domain in the plume, which they referred to as the 'inner sphere'. According to Ref. [11], only this domain, which corresponds to a denser and hotter plasma and is located close to the target surface but does not contact with it, is the source of glow in the form of a spectral continuum and discrete lines belonging to the ions of the target material. The data obtained in the present work show that the radiating buffer gas atoms are also localised, at least in the surface layers of this domain. At the same time, it is precisely for this plasma domain that our experiment yields the lowest electron temperatures (see Fig. 2). It would be natural to ascribe the brightly glowing domain in the vaporised material cloud to the dense plasma whose propagation is limited by the contact surface with the buffer gas. In a supersonic flow, the discontinuity of gas-dynamic parameters falls on a contact surface, like on the shock front, and the condition of local thermal equilibrium is not fulfilled on this surface. It is likely that this is the reason for the dip in the distance dependences of T_e at 500–1500 μm from the target surface. At longer distances from the surface the plasma expansion is subsonic; in this case, T_e passes through a maximum. We note that T_e is also appreciably higher in the plasma layer, which is up to 300 μm in thickness, located in the immediate vicinity of the surface. A one-dimensional approximation applies to the shock propagation through this layer. In the absence of nonstationary gas-dynamic motion (of the shock and of the contact surface) along the target surface, only subsonic plasma flow may occur along the target surface, which is also realised at distances exceeding the run of the contact surface along the axis of the plasma cloud.

3.2. Profiles of the spectral lines of the buffer gas

The spectral lines of copper atoms shown in Fig. 1 exhibit symmetrical profiles, which agree nicely with the Lorentzian profiles represented by the dotted curve. The lines of argon exhibit the same symmetric profile in the irradiation under regime 3. A substantially different shape is typical for buffer gas lines in the target ablation under regimes 1 and 2 at pressures exceeding the percolation threshold. Figure 4 shows the experimental profile of a helium line (λ_{He} = 587.6 nm), obtained at a pressure of 10 atm, as well as the results of its approximation by one and two Lorentzian profiles. In the latter case, which provides a more accurate description of the experiment, one of the profiles has a small width typical for the helium line at a low pressure, whereby there applies a single-Lorentzian approximation. The other Lorentzian, the

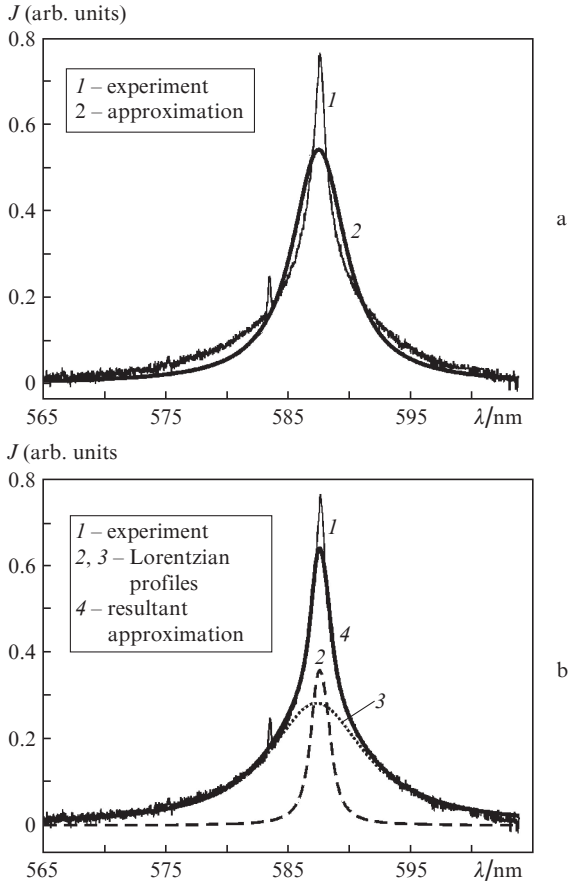

Figure 4. Experimental profile of the λ_{He} = 587.6 nm line and results of approximation by one (a) and two (b) Lorentzian profiles (regime 1). Target: Re.

broader one, is realised at pressures which exceed the threshold value for percolation and, as we believe, may arise from helium atoms that find themselves near a percolation cluster. Similar changes occur to the lines of atomic argon and hydrogen under regime-1 exposure.

Presented below are dependences for the one-Lorentzian approximation for buffer gas lines. As follows from Fig. 4, when the experimental profile of a helium line is decomposed into two profiles, the width of the narrow profile turns out to be approximately 2.5 times narrower and the width of the broad one 3.5 times narrower than the width of the profile of one-Lorentzian approximation.

3.3. Spectral line broadening in relation to the distance from the target surface

Figures 5 and 6 show the intensity and width of discrete lines in the plasma spectrum as functions of distance from the target in the ablation under regime 1. These data were obtained in the expansion of magnesium vapour in the surrounding buffer gas (He) at a pressure of 5 atm close to the percolation threshold. The plasma and the buffer gas are separated by the contact surface, which appreciably lags behind the shock front [13, 14]. Upon the damping of the explosion wave and the slowing-down of the contact surface, the plasma expansion continues, though without gas-dynamic discontinuities of the physical parameters, for instance of the ionisation degree. The plasma front becomes diffuse, the electron plasma density becomes lower. The spectral line widths of He I and Mg I as well as their integral intensities peak at the same distance from the target surface equal to ~700 μm (see Figs 5 and 6), which should be attributed to the path of the contact surface. We note that the curves in Fig. 5 are normalised to the peak width of the corresponding line. At the same time, a significant feature is observed for the integral intensity of atomic magnesium spectrum, which abruptly increases at the distance specified above and then vanishes at an almost two times longer distance (see Fig. 6). The wider existence domain of excited magnesium atoms in comparison with helium could be attributed to the difference in their excitation mechanisms: the thermal process for Mg versus the process responsible for the excitation of electrons to the He I excitation energy. The abrupt growth of the integral intensities in Mg I spectrum testifies to the fact that the relative density of single magnesium ions increases appreciably in going over to a free plasma expansion. The natural assumption that the intensity growth of Mg I spectrum is due to the recombination between Mg II ions and electrons is not borne out by the data given in Fig. 5. Recombination does not affect the widths of Mg I and He I lines, which depend linearly on the electron density. Conceivably the growth of Mg I density results from the vaporisation (disintegration) of percolation clusters, which consist of virtually coupled magnesium atoms, near the percolation threshold.

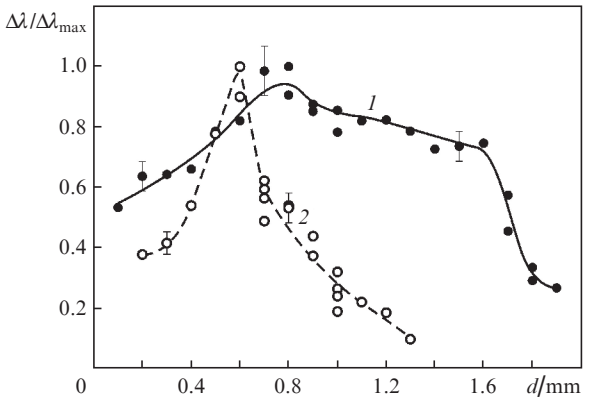

Figure 5. Widths of Mg I (*1*) and He I (*2*) spectral lines as functions of the distance from the surface of a magnesium target at a buffer gas (He) pressure of 5 atm (regime 1).

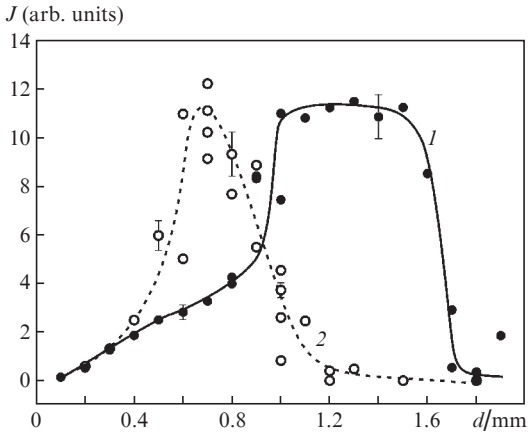

Figure 6. Dependences of the intensity of Mg I (*1*) and He I (*2*) spectral lines on the distance from the surface of a magnesium target at a buffer gas (He) pressure of 5 atm (regime 1).

3.4. Broadening of spectral lines in relation to the pressure

The damping of the explosion wave and therefore the position of the peaks of the characteristics shown above depend on the initial buffer gas pressure. Naturally, in the measurement of the pressure dependence of the width, account should be taken of its dependence on the distance from the target. In the present work, initially for each pressure value we measured the distance dependence of the width of the spectral line of a buffer gas, and its maximum value was employed for constructing the pressure dependence.

The curves in Figs 7 and 8 serve to illustrate the variation of the spectral linewidths of the buffer gases and the target material under variation of the initial buffer gas pressure (density). Metal targets were ablated under regime 1, the glow was recorded in the direction perpendicular to the direction of plume expansion. We compare the broadening of the atomic lines of argon (λ_{Ar} = 696.5 nm) and copper (λ_{Cu} = 521.8 nm) in Fig. 7 and the broadening of the lines of helium (λ_{He} = 587.6 nm) and hydrogen (λ_H = 656.3 nm, the H_α line of the Balmer series) in Fig. 8. A special feature of the broadening of the lines of buffer gases is its threshold character, which manifests itself either as the glow of a buffer gas (for Ar) or as a sharp increase in dJ/dp, where J is the spectral line intensity, on attaining the threshold pressure. The threshold pressure, which is marked with an arrow in the figures, does not manifest itself in the broadening of the lines of the target material. Also shown in Fig. 7 is the pressure dependence of the integral intensity of the spectral line of copper. Observed in the above-threshold pressure range is a dip, which results from the lowering of the density of single atoms of the target material arising from cluster formation.

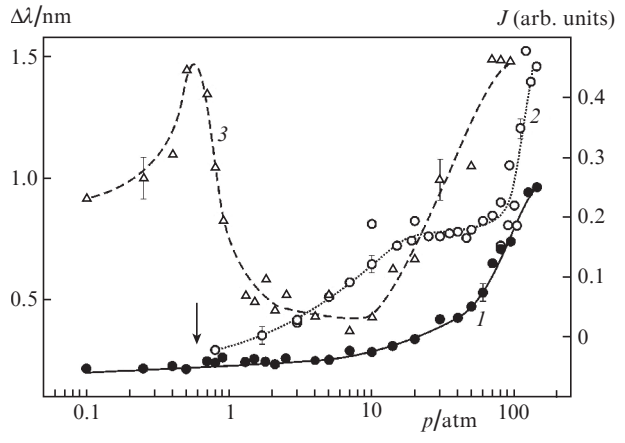

Figure 7. Dependences of the spectral linewidths of Cu I (*1*) and Ar I (*2*) and the Cu I line intensity (*3*) on the buffer gas pressure (regime 1).

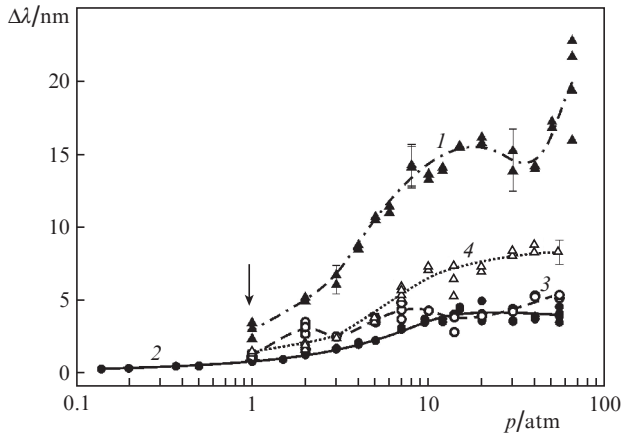

Figure 8. H I (*1*, *3*) and He I (*2*, *4*) spectral linewidths as functions of buffer gas pressure [(*1*) and (*2*) pure gas, (*3*) and (*4*) hydrogen-helium ratio of 1 : 10]. Target: Re. Regime 1.

The pressure dependences depicted in Fig. 8 were obtained in the ablation of a Re target in the atmosphere of pure hydrogen and helium buffer gases as well as of their mixture with their partial pressure ratio of 1 : 10. For a low hydrogen density in the buffer atmosphere the H_α linewidth turns out to be significantly (by about 3.3 times) smaller than in pure hydrogen. By contrast, the helium line is 1.7 times broader than in pure helium. The observed changes in plasma electron density are evidently due to the ionisation of hydrogen atoms.

In accordance with the quasistatic model of Stark broadening, the following approximations apply to hydrogen-like and nonhydrogen-like atoms [15, 16]:

$$\Delta\lambda_H \approx C(n_e)^{2/3}, \quad (1)$$

$$\Delta\lambda = 2w_e(1 + g\alpha_N)n_e \times 10^{-16} \approx 2 \times 10^{-16} w_e n_e, \quad (2)$$

where w_e is the parameter for electron broadening (Å); n_e is the electron plasma density (cm^{-3}); and $\Delta\lambda$ is the half-height linewidth (Å). The factor $\alpha_N = \alpha n_e^{0.25} \times 10^{-4}$ characterises the ion contribution to the broadening [parameters w_e and α are given in Ref. [15], and the factor $g = 1.75(1 - 0.75R)$] defines the role of Debye screening (parameter R is the ratio between the average inter-ion distance and the Debye length). Formula (2) holds good when $\alpha < 5 \times 10^3 n_e^{0.25}$ [15, 16].

Classical formula (1) with the constant $C \approx 5.4 \times 10^{-11}$ for the H_α line holds in the range of relatively low densities and temperatures. When the density $n_e \geqslant 10^{18}$ cm^{-3}, the coefficient in formula (1) increases by about 50% due to several effects [17], with the result that the electron density determined from the broadening of spectral lines lowers by 30%. Considering the complex lineshape approximated by two profiles, this correction may be neglected. In the case of nonhydrogen-like buffer gas atoms, for the same reason it is possible to use single-profile lineshape approximations and approximation (2), which overrates the density for $n_e \geqslant 10^{18}$ cm^{-3}.

For the $\lambda_{He} = 587.6$ nm helium line, the parameter w_e(He) ≈ 0.17 Å [15]. According to formula (2), a half-width $\Delta\lambda_{He} =$ 10 nm results from the electron density $n_e \approx 2 \times 10^{18}$ cm^{-3} in the plasma domain which contains radiating helium atoms. For the copper line ($\lambda_{Cu} = 521.8$ nm, $\Delta\lambda_{Cu} = 1$ nm, w_e(Cu) $\approx$ 0.08 Å [18]), for the same ~10-atm pressure (see Fig. 7) we obtain one order of magnitude lower density, $n_e \approx 3 \times 10^{17}$ cm^{-3}. Being a buffer gas, helium is present in front of the contact surface, where the electron density is relatively low [19]. The main contribution to the integral intensity of helium lines, as one may assume, was made by the atoms which found themselves in the immediate vicinity of the contact surface. By contrast, in the discrete copper spectrum the contribution was made entirely by the atoms which left that domain occupied by a relatively dense plasma.

Therefore, the width and shape of the atomic spectral lines of the target substance irradiated by a single pulse correspond to the plasma domain located in front of the moving contact surface. The radiation of buffer gas spectra originates in a denser plasma layer. Interestingly, the radiation arising from the atoms of the target substance is not observed from this layer. Unlike the buffer gas, no significant change of atomic line profiles was observed for the target substance. We emphasise that a markedly greater line broadening in the atomic substance spectrum is observed under exposure to a millisecond pulse (see Fig. 1), whereby a fractal shell is formed in the cool outer plasma layers [8].

4. Conclusions

For the first time we compared the broadening of the spectral lines of a buffer gas and the target substance in the plasma generated in laser ablation. The experimental investigation was carried out for different targets and their ambient atmospheres. The pressure dependence of the spectral linewidth of the buffer gas was found to be qualitatively different from the corresponding dependence in the spectrum of the target substance. The threshold behaviour typical for the spectral lines of the buffer gas is accompanied by changes of its profile, which is most likely due to the strong electron density gradient in the plasma domain which harbours the radiating rare-gas atoms. The formation of percolation clusters behind the contact surface, on the one hand, lowers the intensity of the atomic spectrum of the target substance and, on the other, increases the intensity of the spectral lines of the buffer gas and results in their broadening.

References

1. Zhukhovitskii D.I. *Zh. Eksp. Teor. Fiz.*, **113**, 181 (1998) [*JETP*, **86**, 101 (1998)].

2. Ozhovan M.I. *Zh. Eksp. Teor. Fiz*., **104**, 4021 (1993) [*JETP*, **77**, 939 (1993)].
3. De Freitas J.S., Lucena L.S., Roux S. *Physica A*, **266**, 81 (1999).
4. Smirnov B.M. *Usp. Fiz. Nauk*, **170**, 495 (2000) [*Phys. Usp*., **43**, 453 (2000)].
5. Baskin E.M., Entin M.V., Sarychev A.K., et al. *Physica A*, **242**, 49 (1997).
6. Sarychev A.K., Shubin V.A., Shalaev V.M. *Phys. Rev. E*, **59**, 7239 (1999).
7. Konjevic N. *Plasma Sources Sci. Technol.*, **10**, 356 (2001).
8. Kask N.E., Leksina E.G., Michurin S.V., Fedorov G.M., Chopornyak D.B. *Kvantovaya Electron*., **32**, 437 (2002) [*Quantum Electron*., **32**, 437 (2002)].
9. Mao X.L., Shannon M.A., Fernandez A.J., Russo R.E. *Appl. Spectrosc.*, **49**, 1054 (1995).
10. Man B.Y., Dong Q.L., Wei X.Q., et al. *J. Opt. A: Pure Appl. Opt*., **6**, 17 (2004).
11. Lee Y.-I., Song K., Cha H.-K., et al. *Appl. Spectrosc.*, **51** (7), 959 (1997).
12. Hafez M.A., Khedr M.A., Elaksher F.F., Gamal Y.E. *Plasma Sources Sci. Technol.*, **12**, 185 (2003).
13. Yusupaliev U. *Zh. Tekh. Fiz.*, **74** (7), 52 (2004).
14. Harilal S.S., Bindhu C.V., Tillack M.S., et al. *J. Appl. Phys*., **93**, 2380 (2003).
15. Griem H. *Spectral Line Broadening by Plasmas* (New York: Academic, 1974; Moscow: Mir, 1978).
16. Kobilarov R., Konjevich N., Popovich M.V. *Phys. Rev. A*, **40** (7), 3871 (1989).
17. Parigger C.G., Plemmons D.H., Oks E. *Appl. Opt*., **42** (30), 5992 (2003).
18. Kasabov G.A., Eliseev V.V. *Spektroskopicheskie tablitsy dlya nizkotemperaturnoi plazmy* (Spectroscopic Tables for Low-Temperature Plasmas) (Moscow: Atomizdat, 1973).
19. Wien S.B., Mao X., Greif R., Russo R.E. *J. Appl. Phys*., **102**, 043103 (2007).